

# Entropy Injection as a Global Feedback Mechanism

S. Peng Oh & Andrew J. Benson

*Theoretical Astrophysics, Mail Code 130-33, Caltech, Pasadena, CA 91125, USA*

18 November 2018

## ABSTRACT

Both preheating of the intergalactic medium and radiative cooling of low entropy gas have been proposed to explain the deviation from self-similarity in the cluster  $L_X - T_X$  relation and the observed entropy floor in these systems. However, severe overcooling of gas in groups is necessary for radiative cooling alone to explain the observations. Non-gravitational entropy injection must therefore still be important in these systems. We point out that on scales of groups and below, gas heated to the required entropy floor cannot cool in a Hubble time, regardless of its subsequent adiabatic compression. Preheating therefore shuts off the gas supply to galaxies, and should be an important global feedback mechanism for galaxy formation. Constraints on global gas cooling can be placed from the joint evolution of the comoving star formation rate and neutral gas density. Preheating at high redshift can be ruled out; however the data does not rule out passive gas consumption without inflow since  $z \sim 2$ . Since for preheated gas  $t_{\text{cool}} > t_{\text{dyn}}$ , we speculate that preheating could play a role in determining the Hubble sequence: at a given mass scale, high  $\sigma$  peaks in the density field collapse early to form ellipticals, while low  $\sigma$  peaks collapse late and quiescently accrete preheated gas to form spirals. The entropy produced by large scale shock-heating of the intergalactic medium is significant only at late times,  $z < 1$ , and cannot produce these effects.

## 1 INTRODUCTION

Numerical simulations of dark matter halos reveal an almost universal density profile over a wide range of masses (Navarro, Frenk & White 1997; Ghigna et al 2000; Klypin et al 2001; Power et al 2002). If the gas faithfully traced the dark matter, we would expect the bolometric X-ray luminosity to scale with the cluster virial temperature as  $L_X \propto T^2$  (Kaiser 1986), while observations indicate significant steepening of this relation for low-temperature clusters (Helsdon & Ponman 2000, and references therein), suggesting that some non-gravitational process is affecting the properties of the gas. Indeed, observations of the X-ray surface brightness profiles in poor groups reveal the existence of an entropy floor,  $S = T/n_e^{2/3} \sim 100 \text{keVcm}^2$  (Ponman, Cannon, & Navarro 1999), in the gas. Such an entropy floor reduces the central gas density and breaks the self-similarity of gas density profiles. There are two schools of thought as to how this entropy floor could have arisen: (i) as a result of non-gravitational heating of order  $\sim 1 \text{keV}$  per particle, arising from winds driven either by supernovae or active galactic nuclei (e.g., Kaiser 1991; Ponman, Cannon, & Navarro 1999), (ii) as a result of radiative cooling of the low entropy gas, leaving behind only the high entropy gas (which cannot cool within a Hubble time; e.g., Voit & Bryan 2001). Numerical simulations which incorporate either of these schemes can reproduce the observed cluster  $L_X - T$  relation.

In this paper, we critique the first scenario, on the ba-

sis of the disastrous effects the required level of preheating would have on subsequent galaxy formation. Groups and clusters are the most massive non-linear structures present today; to have a significant effect on their gas profile, a large amount of energy must be injected ( $\sim 1 \text{keV}$  per particle). The virial temperature of galaxies is much smaller (for an  $L_*$  galaxy, typically  $T_{\text{vir}} \sim 0.1 \text{keV}$ ); galaxies will therefore be unable to accrete gas heated to such high entropies. Furthermore, we shall show that the gas they do manage to accrete cannot cool within a Hubble time. The net effect would be a sharp downturn in the comoving star formation rate. Mo & Mao (2002) have also recently examined the impact of preheating on galaxy formation; they find that preheating could have a strong impact on the X-ray luminosity and morphology of galaxies. However (unlike the present work), they do not consider if preheating will suppress subsequent star formation. Throughout, we assume a cosmology where  $(\Omega_m, \Omega_\Lambda, \Omega_b h^2, h, \sigma_{8h^{-1}}) = (0.3, 0.7, 0.019, 0.7, 0.9)$ , consistent with current observational constraints (e.g. Netterfield et al 2002; Freedman et al 2001; Smith et al 2002).

## 2 THE IMPACT OF PREHEATING ON GAS COOLING

### 2.1 The overcooling problem

Recently, it has been pointed out in semi-analytic work (Bryan 2000; Voit & Bryan 2001; Voit et al 2002) and

numerical simulations (Lewis et al 2000; Muanwong et al 2002; Davé et al 2002) that radiative cooling could be responsible for the observed entropy floor in groups and clusters. Here we point out that: (i) radiative cooling without non-gravitational feedback likely results in severe overcooling of gas at group scales, where the entropy floor is most clearly seen. (ii) Depending on its magnitude and redshift of injection, an entropy floor due to preheating can efficiently regulate overcooling in groups. Thus, some form of preheating is still likely to be necessary. This does not preclude an important role for radiative cooling: it reduces the otherwise severe energetic requirements for preheating, since the lowest entropy gas simply cools, rather than being heated up to the entropy floor.

Let us calculate the amount of cooled gas in the absence of feedback, as a function of halo mass. Unlike other semi-analytic models, we also wish to consider a dynamic model in which gas is drawn inward and compressed within a cooling flow, rather than a static model in which all gas is cooled out to some cooling radius. This is so as to explicitly check that the increased gas densities due to inward flow do not significantly increase cooling rates and thus the cooled mass fraction. We therefore perform 1D spherically symmetric calculations very similar to that of Tozzi & Norman (2001), who compute a sequence of adiabats generated by the accretion shock and follow their subsequent evolution due to radiative cooling; refer to Tozzi & Norman (2001) for more details on such models. This is an implicitly Lagrangian scheme and allows us to directly track the entropy evolution of each mass shell. The main difference between our treatment and theirs is that we only implement gas cooling within a static potential, rather than an evolving potential; experimentation has found that this makes little difference. We also consider the dark matter to impose a fixed potential, and ignore the self-gravity of the gas.

We approach the problem by considering the sequence of adiabats through which a gas shell evolves. The initial entropy profile of the gas as a function of the mass profile,  $K(M) \equiv P(M)/\rho(M)^\gamma = k_B T/\mu m_p \rho^{2/3}$ , can be determined by using the shock jump conditions if the temperature and density at the accretion shock are known. We assume the dark matter distribution follows an NFW profile (Navarro, Frenk, & White 1997). We assume a perfect gas,  $P = \frac{\rho}{\mu m_H} k_B T$ , and a polytropic equation of state,  $P = K\rho^\gamma$ , where  $\gamma = 5/3$ . Tozzi & Norman (2001) find that the average growth of the main progenitor of the dark matter halo, found by running Monte Carlo realizations based on the extended Press-Schechter formula (e.g., Lacey & Cole 1993), can be approximated by the formula:  $m(z) = \left(\frac{1+z}{1+z_0}\right)^{-[B+A \log\left(\frac{1+z}{1+z_0}\right)]}$ , where  $A$  and  $B$  depend on cosmology, the final mass  $M_0$ , and the observed redshift  $z_0$  (we consider  $z_0 = 0$  in this paper). As a function of  $(M_{\text{DM}}, z)$  the infall velocity is then found from:

$$\frac{v_i^2}{2} = \frac{v_{\text{ff}}^2}{2} + \Delta W - \frac{c_s^2}{\gamma - 1} \left[ \left( \frac{\rho_{\text{ta}}}{\rho_e} \right)^{\gamma-1} - 1 \right], \quad (1)$$

where  $\frac{v_{\text{ff}}^2}{2} = \frac{GM}{R_s} - \frac{GM}{R_{\text{ta}}}$  ( $R_s \approx R_{\text{vir}}$  is the shock radius, and  $R_{\text{ta}} \approx 2R_{\text{vir}}$  is the turnaround radius),  $\rho_e$  is the external

preshock density at  $R = R_s$ , and  $c_s = (\gamma K_{\text{IGM}} \rho_e^{\gamma-1})^{1/2}$  is the sound speed where  $K_{\text{IGM}}$  is the preshock entropy of the IGM gas being accreted. The postshock temperature is then given by (Landau & Lifshitz 1957; Cavaliere, Menci & Tozzi 1998):

$$k_B T_i = \frac{\mu m_p v_i^2}{3} \left[ \frac{(1 + \sqrt{1 + \epsilon})^2}{4} + \frac{7}{10} \epsilon - \frac{3}{20} \frac{\epsilon^2}{(1 + \sqrt{1 + \epsilon})^2} \right], \quad (2)$$

where  $\epsilon \equiv 15 k_B T_e / 4 \mu m_p v_i^2$ . The postshock density is given by  $\rho_i = g \rho_e$ , where the shock compression factor  $g$  is given by (Cavaliere, Menci, & Tozzi 1997):

$$g = 2 \left( 1 - \frac{T_e}{T_i} \right) + \left[ 4 \left( 1 - \frac{T_e}{T_i} \right)^2 + \frac{T_e}{T_i} \right]^{1/2}. \quad (3)$$

From this one can compute the postshock adiabat

$$K_{\text{shock}} = k_B T_i / \mu m_p \rho_i^{\gamma-1}. \quad (4)$$

We have also computed the entropy profiles assuming that the gas traces the NFW profile and is in hydrostatic equilibrium, a model used by Voit et al (2002). We have found that the entropy profile computed with either model is very similar; both are sharply increasing functions of radius. We have also found that the entropy profile for different cluster masses (scaled to the entropy of the outermost shell) is fairly self-similar across different cluster masses. This is not surprising, since density and temperature profiles are fairly self-similar in these models; they only differ to the extent that their central concentration (which depends primarily on the collapse redshift) varies. We will examine the effects of an entropy floor in these models in §2.2.

Given an initial entropy profile  $K(M, t = 0)$ , we simultaneously solve the equations for the variables  $K(M, t)$ ,  $\rho(M, t)$ ,  $R(M, t)$  (which automatically also yields  $T(M, t) = K(M, t) \rho(M, t)^{\gamma-1} \mu m_H / k_B$ ):

$$\begin{aligned} \frac{dP}{dM_{\text{gas}}} &= -\frac{GM_{\text{DM}}}{4\pi r^4} \\ \frac{dr}{dM_{\text{gas}}} &= \frac{1}{4\pi \rho_{\text{gas}} r^2} \end{aligned} \quad (5)$$

Given the initial entropy profile we have calculated, we can compute the initial pressure profile of the gas, if we assume the boundary condition  $\rho(R_{\text{vir}}) = f_B \rho_{\text{NFW}}(R_{\text{vir}})$ , where  $f_B = \Omega_b / \Omega_m$  is the universal baryon fraction. The pressure and entropy profile fully specify the initial density and temperature profile of the gas. We now allow for radiative cooling to operate, and update the entropy profile via:

$$\frac{d}{dt} \ln(K) = -\frac{1}{\tau_{\text{cool}}(K)}, \quad (6)$$

where the cooling time is:

$$\tau_{\text{cool}} \equiv \frac{3}{2} \frac{k_B T}{\Lambda_N} \frac{\rho_{\text{gas}}}{\mu m_p}, \quad (7)$$

and we use a fit given by Tozzi & Norman (2001) to the cooling function  $\Lambda_N$  of Sutherland & Dopita (1993), which includes both free-free and line emission, for a metallicity of  $Z = 0.3Z_\odot$ . We choose our timestep so that it corresponds to the cooling time of the third innermost shell; this is sufficient to obtain convergent results without excessively long

computation times. As gas cools and drops out at the center, an inward cooling flow develops. After each timestep, we recompute hydrostatic equilibrium in equation (5) according to the new profile of adiabats  $K(M)$ , updating the density and temperature profile of the gas. Any gas which has cooled below  $T \sim 5 \times 10^5 \text{ K}$  is removed from the calculation and placed in a cold phase at the center of the cluster; we track  $M_{\text{cool}}$  and  $M_{\text{hot}} = M_{\text{gas},0} - M_{\text{cool}}$ . We do not consider distributed mass drop-out in this calculation. When recomputing hydrostatic equilibrium, we use the boundary conditions:

$$\begin{aligned} r(0) &= 0 \\ r(M_{\text{hot}}) &= r_{\text{end}} \\ \rho(M_{\text{hot}}) &= \left[ \rho_{\text{vir}}^{\gamma-1} + \frac{\gamma-1}{\gamma K_{\text{vir}}} \int_{r_{\text{vir}}}^{r_{\text{end}}} -\frac{GM_{\text{DM}}(r)}{r^2} dr \right]^{1/(\gamma-1)} \end{aligned} \quad (8)$$

where  $\rho_{\text{vir}} = \rho_o(r_{\text{vir}})$ ,  $K_{\text{vir}} = K(r_{\text{vir}})$  are the initial density and entropy of the outermost mass shell. The last boundary condition uses the fact that the outermost shell is compressed adiabatically during the inward flow, since for this shell,  $t_{\text{cool}} \gg t_H$ . Note that since we have 3 boundary conditions for 2 ordinary differential equations, we can solve for  $r_{\text{end}}$ , which is an eigenvalue of the problem. Since this is a boundary value problem, we use relaxation to solve the equations. The results of our calculations agree very well with those of Tozzi & Norman (2000), although they use a slightly different set of equations and boundary conditions. In our calculation, we assumed the dark matter potential was fixed and merely evolved the equations for a Hubble time, allowing the gas to cool. We have also experimented with a growing dark matter potential; the results do not differ significantly.

In Figure 1, we show the fraction  $f_{\text{cool}}$  of gas which cools in a Hubble time in our models without preheating, computed according to the convention:

$$f_{\text{cool}} = \frac{M_{\text{cool}}}{M_{\text{tot}}} \frac{\Omega_m}{\Omega_b}, \quad (9)$$

where  $M_{\text{cool}}$  is the mass in the cool phase and  $M_{\text{tot}}$  is the total gravitating mass. We prefer this to the other widely used convention:  $f_{\text{cool}} = M_{\text{cool}}/(M_{\text{cool}} + M_{\text{hot}})$ , where  $M_{\text{hot}}$  is the gas mass in the hot phase, because the total gas mass  $M_{\text{hot}} + M_{\text{cool}}$  in a fixed halo potential decreases with an increasing entropy floor in preheating scenarios (a high entropy floor hinders shallow potential wells from accreting gas). We also choose to show halo mass rather than the X-ray temperature because for a fixed potential, the emission weighted temperature increases with the entropy floor (since gas at the cluster center, which dominates the X-ray emission, becomes hotter). These conventions allow the clearest depictions of the effect of an entropy floor on gas cooling. Also shown as points is  $f_{\text{cool}}$  inferred from the data of Rousset et al (2000), who compile a list of total stellar mass and total gravitating mass for a sample of X-ray clusters. As in Balogh et al (2001) (see their paper for a very lucid discussion of the overcooling problem), we multiply the total stellar mass by 1.1 to account for gas in atomic and molecular form; we also show the global cooled gas fraction of  $f_{\text{cool}} \sim 5\%$  inferred from the K-band luminosity function by

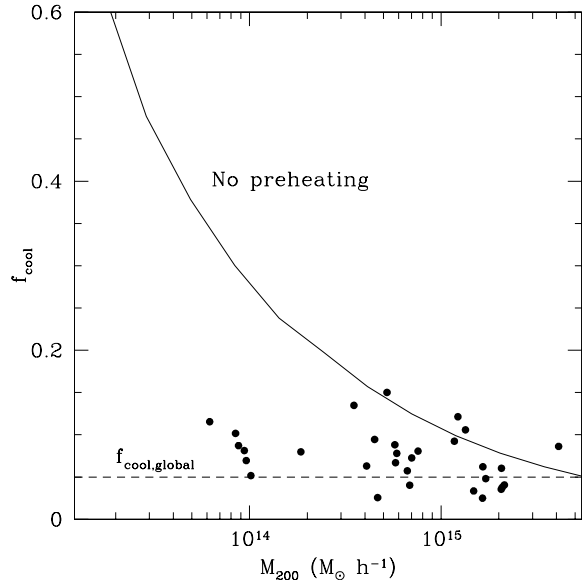


**Figure 1.** The fraction of gas which cools in a Hubble time  $f_{\text{cool}}$  as a function of halo mass, as computed in our models without preheating. The points depict the fraction of baryons in the cold phase in a sample of clusters from Rousset et al (2000). The dashed line shows the best estimate of the global cold baryon fraction from the K-band luminosity function of Cole et al (2001). Radiative cooling alone without feedback results in severe overcooling, particularly in groups.

Cole et al (2001). The latter figure is somewhat lower than the customarily quoted value of  $6\% < f_{\text{cold}} < 17\%$  found by Fukugita, Hogan, & Peebles (1998), but much more robust as it does not depend on the highly uncertain relative abundances of galaxies of different morphological types, which have very different  $M/L_B$ ; by contrast  $M/L_K$  varies by at most a factor of two over different stellar population histories (Bell & de Jong 2000).

We see that while radiative cooling alone may be consistent with observations in the most massive clusters, severe overcooling of the gas would occur on group scales and below if radiative cooling alone were to operate without feedback, with  $\sim 50\%$  of the gas entering the cold phase. In our models we have computed the entropy profiles and allowed for gas inflow and compression in a cooling flow. We also computed static models which assume that the gas traces the dark matter and that all gas cools out to some cooling radius  $r_{\text{cool}}$  where  $t_{\text{cool}} \sim t_H$  (White & Frenk 1991; Voit et al 2002; Wu & Xue 2002), and obtained very similar results. We comment on this robustness in §2.2.

This overcooling effect is in fact consistent with all numerical simulations which claim to explain the observed  $L_X - T_X$  relation from the effects of radiative cooling alone, although this has not been sufficiently emphasized. For instance, while Muanwong et al (2002) find a global cooled gas fraction of  $f_{\text{cool}} \sim 15\%$ , on group scales where  $M_{\text{vir}} \sim \text{few} \times 10^{13} M_\odot h^{-1}$ , the cooled mass fraction is  $f_{\text{cool}} \sim 30 - 50\%$  (see their Figure 3). Davé et al (2002) find that while  $f_{\text{cool}} \sim 24\%$  globally in their simulations, for

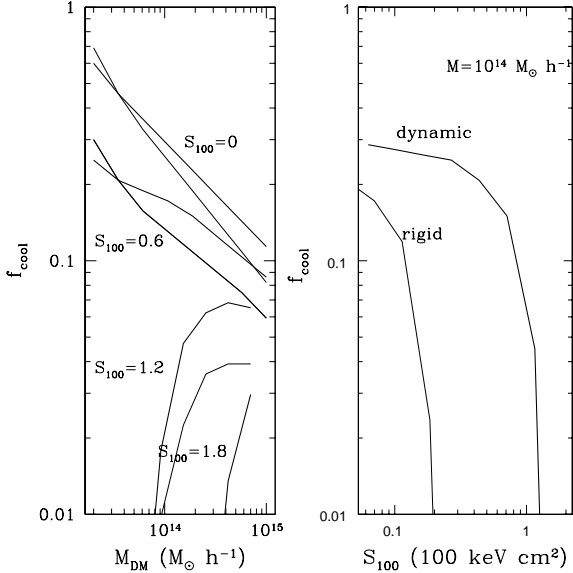


**Figure 2.** The effect of an entropy floor  $S_{100}$  on the cool gas fraction  $f_{\text{cool}}$  as given by equation 9. As the entropy floor increases, the fraction of gas able to cool in a Hubble time falls drastically. We track the inward flow and compression of the gas as it cools (dark solid lines); however, ignoring the work done on the gas by the gravitational potential and assuming it is static gives very similar results (light solid lines).

halos with  $\sigma_{1D} \sim 100 \text{ km s}^{-1}$ , then  $f_{\text{cool}} \sim 80\%$ , while for halos with  $\sigma_{1D} \sim 500 \text{ km s}^{-1}$ , then  $f_{\text{cool}} \sim 50\%$ ; for these extreme levels of gas cooling, consistency with the observed  $L_X - T_X$  relation can be achieved. The overcooling problem is often dealt with in numerical simulations by deliberately restricting the resolution to  $\sim 10^{11} M_{\odot}$ ; all simulations of higher resolution generically suffer from overcooling (Balogh et al 2001), as was pointed out by Suginozawa & Ostriker (1998). Based on the Mulchaey et al (1996) sample, Bryan (2000) claims that the cool gas fraction increases from cluster to groups scales, and consistency with the radiative cooling model can be achieved. However, he computed  $f_{\text{cool}} = M_{\text{cool}} / (M_{\text{cool}} + M_{\text{hot}})$ , and estimates of the hot gas component are likely to be systematically biased downwards in groups due to the limited radial extent of the X-ray profile (Roussel et al 2000).

We therefore contend that radiative cooling alone as an explanation for the observed scaling relations and entropy floor in groups and clusters is untenable. The problem is most acute in groups: since most of the gas in groups is at comparatively low entropy, a larger fraction of the gas has to cool to recover the observed entropy floor. In the next section we explore how entropy injection can ameliorate the overcooling problem.

## 2.2 The Effect of an Entropy Floor on Gas Cooling

Let us now suppose that some form of external preheating takes place, in which the IGM is boosted to some en-

tropy floor  $K_{\text{IGM}}$ . What is the effect of this entropy floor on gas cooling? We can easily incorporate the effects of a pre-existing entropy floor into our models. If the infall velocity does not exceed the local sound speed, then the gas is accreted adiabatically and no shock occurs; the gas entropy  $K_{\text{IGM}}$  is therefore conserved. If gas infall is supersonic, then the gas is shocked to the entropy  $K_{\text{shock}}$  computed in the previous section. Tozzi & Norman (2001) found that the transition between the adiabatic accretion and shock heating regime is very sharp. Thus to a very good approximation we can set  $K(M) = \max(K_{\text{shock}}(M), K_{\text{IGM}})$ ; with this new entropy profile we can compute density and temperature profiles and gas cooling properties as before. Similar to previous work (e.g., Tozzi & Norman 2001; Voit et al 2002), we find that an entropy floor creates a core in the density profile, decreasing the central density and increasing the central temperature.

Let us define, as is customary, the entropy parameter  $S \equiv T/n_e^{2/3}$ , and

$$S_{100} \equiv \left( \frac{S}{100 \text{ keV cm}^2} \right). \quad (10)$$

For mean molecular weight  $\mu = 0.6$ , this is related to our previously defined entropy parameter in equation (4) via  $S_{100} = 6.27 K_{34}$ , where  $K_{34} = 10^{34} \text{ erg cm}^2 \text{ g}^{-5/3}$ . Typical values of the observed entropy floor range between  $S_{100} \sim 1$  (Ponman, Cannon, & Navarro 1999), to  $S_{100} \sim 4$  (Finoguenov et al 2002). Only values toward the lower end of such estimates can be produced by radiative cooling alone (Voit & Bryan 2001), whereas values toward the higher end are necessary to reproduce the observed  $L_X - T_X$  relation (Tozzi & Norman 2001).

In Figure 2, we show how the cool gas fraction  $f_{\text{cool}}$  varies with the entropy floor  $S_{100}$ . We see two main features in this plot: (i) an increase in the entropy floor drastically decreases the cooled gas fraction. An entropy floor thus has the potential to solve the overcooling problem. (ii) The results of the calculation where the inward flow and compression of the gas as it cools is tracked (dark solid lines) is very similar to the case when this is ignored and the gas is assumed to be static (light solid lines). The compression of the gas by the gravitational potential as it flows inwards only causes a mild increase in the final cooled gas fraction  $f_{\text{cool}}$ ; naively, one might have expected that the increased densities would result in much more rapid cooling.

To understand these results, let us consider how gas cooling times evolve at fixed entropy. If gas with entropy  $S_{100}$  evolves adiabatically, the gas temperature depends on its density as:

$$T = 4.7 \times 10^4 S_{100} \delta^{2/3} (1+z)^2 \text{ K}, \quad (11)$$

where  $\delta = n_e/\bar{n}_e$  is the overdensity of the gas. The isobaric cooling time is then:

$$\begin{aligned} t_{\text{cool}} &= \frac{5n_e k_B T}{2\mu n_e \Lambda(T)} \propto S^{3/2} (T < 10^7 \text{ K}) \\ &\propto \frac{S^{1/2}}{n^{2/3}} (T > 110^7 \text{ K}) \end{aligned} \quad (12)$$

where  $\mu \approx 0.6$  is the mean molecular weight. We have used  $\Lambda(T) \propto T^{1/2}$  for  $T > 10^7 \text{ K}$  (free-free cooling dominated

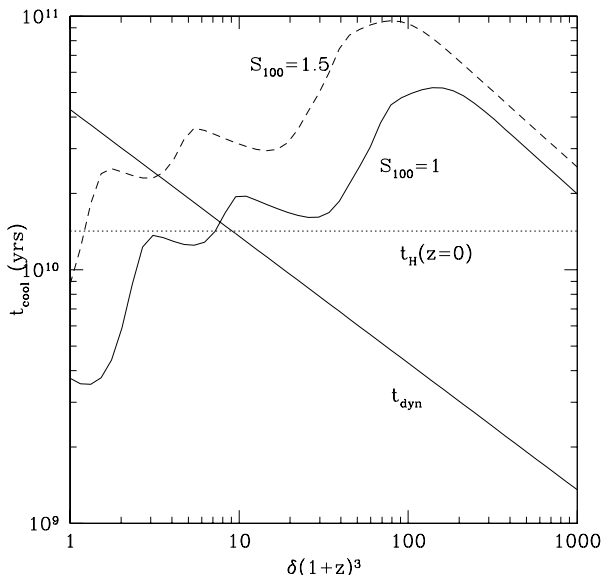


**Figure 3.** The cooling time as a function of density  $n = 2 \times 10^{-7} \delta(1+z)^3 \text{ cm}^{-3}$  for gas at fixed entropy  $S_{100}$ , as defined in equation 10. Also shown are the Hubble time at  $z=0$  and the dynamical time  $t_{\text{dyn}} \propto n^{-1/2}$ . The cooling time depends only weakly on density; for the range of temperatures relevant for galaxy-sized halos,  $T < 0.1 \text{ keV}$  or  $\delta(1+z)^3 < 100 S_{100}^{3/2}$ , it typically *increases* with density. In general, gas above the entropy floor  $S > S_{100}$  cannot cool in a Hubble time.

regime) and  $\Lambda(T) \propto T^{-1/2}$  for  $10^{5.5} \text{ K} < T < 10^7 \text{ K}$  (line cooling dominated regime). We can explicitly compute the cooling time as a function of density for a fixed adiabat; the results are shown in Figure 3. We have used a fit (Nath 2002) to the Sutherland & Dopita (1993) cooling function, assuming that  $Z = 0.3 Z_{\odot}$ ; the detailed temperature dependence of the cooling function in the line cooling dominated regime is not strictly  $\Lambda \propto T^{-1/2}$ , which is why there is a weak density dependence in the cooling time at low density. The most important feature to note is that gas above a certain entropy floor  $S_{\text{crit}} > S_{100}$  cannot cool in a Hubble time, regardless of its density and/or how it is adiabatically compressed. It is thus easy to understand how an entropy floor drastically decreases the cool gas fraction  $f_{\text{cool}}$  as  $S_{\text{preheat}} \rightarrow S_{\text{crit}}$ . We can also understand why the compression of gas in an inward cooling flow has little effect on  $f_{\text{cool}}$ : the cooling rate depends on the entropy of the gas, not the density. We show this effect in Fig. 4, which shows how the gas density, temperature and cooling time evolve as a gas parcel at fixed entropy is brought inwards. Because gas at large radii is at high entropy, an inward flow only brings about modest compression; the rise in temperature offsets the cooling rate increase due to the increased density, and overall the cooling time only shows a very modest decrease.

The fact that the observed ‘entropy floor’,  $S_{\text{preheat}}$ , corresponds to a critical entropy where  $t_{\text{cool}} > t_H$  is perhaps unsurprising: if  $t_{\text{cool}}(S_{\text{preheat}}) < t_H$ , then we might expect radiative cooling to erase all evidence for an entropy floor. Indeed, it was the central insight of Voit & Bryan (2001)

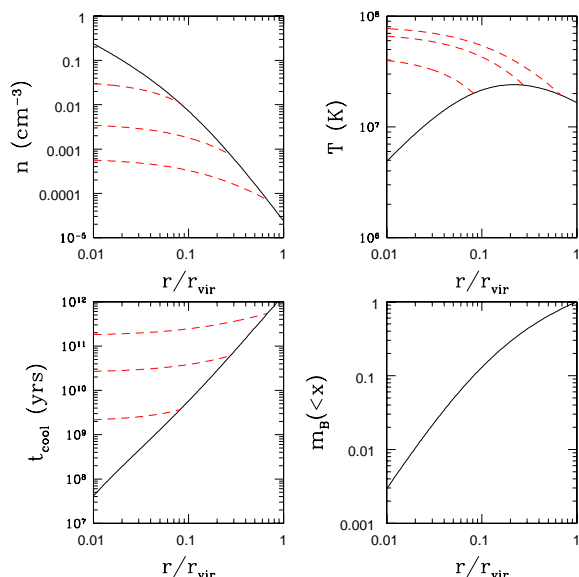


**Figure 4.** Evolution of the density, temperature and cooling time as a parcel of gas is brought inwards adiabatically in a  $M_{\text{DM}} = 10^{14} M_{\odot} h^{-1}$  halo. Because gas at large radii is at high entropy, an inward flow only brings about modest compression; the rise in temperature offsets the cooling rate increase due to the increased density, and overall the cooling time only shows a modest decrease. In fact, for adiabatic compression the cooling time is almost independent of the density, and depends only on the entropy.

that since  $t_{\text{cool}}(S_{\text{crit}}) \sim t_H$ , the entropy floor could have arisen from a floor in the radiative cooling time, rather than an epoch of preheating. However, these statements have very interesting consequences for gas cooling in smaller halos associated with  $L \leq L^*$  galaxies. For the temperature regime we are interested in ( $T \leq 0.1 \text{ keV}$ , or  $\delta < 100 S_{100}^{3/2} (1+z)^{-3}$ ; gas hotter than this cannot be accreted by galaxies), the cooling time either stays constant or *increases* with density for isentropic gas, rather than decreasing with density. Thus, regardless of its final density profile, gas which is accreted adiabatically into a galaxy-size halo has a fairly constant cooling time which depends only upon its initial entropy. Gas which ends up bound to halos at low redshift will typically fulfill  $\delta(1+z)^3 > 10$  at all times. *Thus none of the gas which is heated to the entropy floor will be able to cool in a Hubble time in galaxies. Once the entropy floor in the IGM is established, the supply of fresh gas for star formation is cut off.* This is independent of the details of the accretion of gas and halo mergers; in general, shocks due to this processes can only increase the entropy of the gas, not reduce it. Thus, after  $z_{\text{preheat}}$  where the IGM is heated up to some adiabat  $S_{\text{crit}}$ , fresh accretion of gas from the IGM is halted. Hereafter, we shall follow through on the logical consequences of the observed entropy floor in groups and clusters, if it arose from an epoch of preheating, to assess whether such a scenario is realistic or not.

### 2.3 Bounds on the epoch of preheating

We can use the value of the entropy floor to obtain a lower bound on the epoch of preheating. The gas must be preheated at a sufficiently high redshift that it is accreted adiabatically: i.e.,  $S_{\text{preheat}} > S_{\text{shock}}$ , where  $S_{\text{shock}}$  is the entropy acquired due to the virialization shock in the absence of preheating. Otherwise, the gas will be shocked to a higher adiabat, erasing the signature of preheating. The entropy acquired at the accretion shock  $S_{\text{shock}} = T/n^{2/3} \propto T_{\text{shock}}(1+z)^{-2}$  where  $T_{\text{shock}}$  increases with time as the depth of the potential well grows. Therefore, without preheating the entropy of freshly accreted gas increased monotonically with time. There is thus a minimum redshift  $z_{\text{preheat}}$  below which preheating leaves no imprint on the entropy profile of a cluster, as the entropy of the gas is boosted above the entropy floor by the strong virialization shock. For a present day cluster of mass  $M_o$ , we can compute its entropy profile if we know its accretion history and mass as a function of redshift  $M(z)$ . We can use this to bound the epoch of preheating: if  $S_{\text{preheat}} \sim 100\text{keVcm}^2$ , then for the median accretion history of groups with  $T \sim 1\text{keV}$  (where the entropy floor is most prominent), the epoch of preheating must be  $z \geq 2$ , when the group acquired its core.

A more detailed calculation can be carried out using the extended Press-Schechter theory. We compute the merging history of several  $10^{14}M_{\odot}$  halos identified at  $z = 0$ , using the algorithm of Cole et al (2000), and locate at each redshift the most massive progenitor. For each progenitor we compute  $S_{\text{shock}}$ , and identify those progenitors for which  $S_{\text{shock}} > S_{\text{preheat}}$ . These progenitors are unaffected by preheating. Therefore we are able to estimate the fraction of clusters whose most massive progenitors are unaffected by preheating as a function of redshift. This fraction is shown in Figure 5. At  $z = 2.2$  approximately 50% of cluster progenitors are affected by preheating, while at  $z = 3$ , approximately 95% of cluster progenitors are affected. Thus, preheating must occur prior to  $z = 2-3$  in order to have a significant effect on the cluster gas.

Similarly, from their sample of 9 groups of galaxies observed with ASCA and ROSAT, Finoguenov et al (2002) conclude from extended Press-Schechter theory that the accreted gas reaches an entropy level of  $400\text{keVcm}^2$  by  $z \sim 2.0 - 2.5$ , while such high entropies were not present at  $z > 2.8 - 3.5$ , implying that preheating happened in a fairly instantaneous fashion at  $z \sim 2 - 3$ .

If the entropy of the IGM was indeed boosted to such high levels at  $z \sim 2$ , this implies that the supply of cold gas to galaxies was shut off at that epoch. Remarkably, in their models of cosmic chemical evolution, Pei, Fall & Hauser (1999) concluded that the data was consistent with no gas inflow since  $z \sim 2$ . However, their models were computed for a flat SCDM model, which has since fallen out of favour. By performing a stripped down version of their models, we can nonetheless ask whether the data are consistent with no gas inflow since  $z_{\text{preheat}}$ . If fresh gas cannot cool, then

$$\dot{\Omega}_{\text{g}} = -\dot{\Omega}_{*}(1 - R), \quad (13)$$

where  $\dot{\Omega}_{\text{g}}, \dot{\Omega}_{*}$  are the comoving densities of cold interstellar gas and stars, all in units of the present critical density,

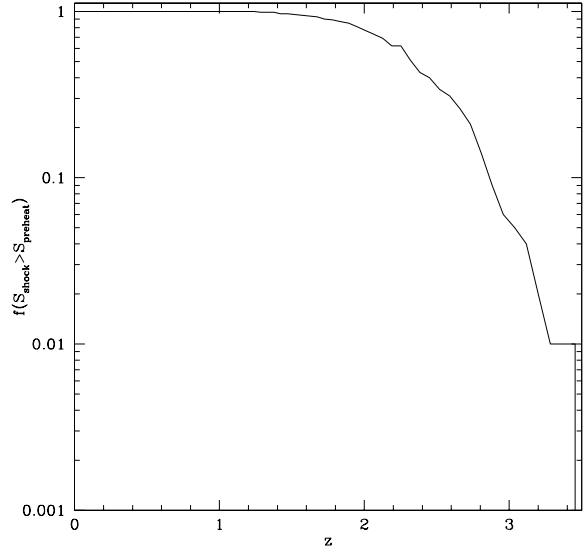


**Figure 5.** The mass fraction of a  $10^{14}M_{\odot}$  halo at  $z = 0$  in halos which are unaffected by a preheating entropy of  $S_{\text{preheat}} = 100\text{keV cm}^2$  as a function of redshift. In order to affect a significant fraction of the cluster’s mass, preheating must occur before  $z \approx 1-2$ .

and  $R$  is the recycled fraction, which is  $0.3 - 0.4$  for typical IMFs. In this case, the comoving gas density at the epoch of preheating is:

$$\Omega_{\text{g}}(z_{\text{preheat}}) = \Omega_{\text{g}}(0) + (1 - R) \int_0^{z_{\text{preheat}}} dz \frac{dt}{dz} \dot{\Omega}_{*}. \quad (14)$$

In principle this is only a lower limit since it neglects outflows due to supernova explosions, galactic winds, etc. To model the evolution of the comoving star formation rate we use a fit to the data from Porciani & Madau (2001) for a  $\Lambda$ CDM cosmology:

$$R_{\text{SFR}}(z) = C(z)h_{65} \frac{\exp(3.4z)}{\exp(3.4z) + 22} M_{\odot}\text{yr}^{-1}\text{Mpc}^{-3}, \quad (15)$$

where  $C(z) = Ah_{65}(\Omega_{\text{m}}(1+z)^3 + \Omega_{\text{k}}(1+z)^2 + \Omega_{\Lambda})^{1/2}/(1+z)^{3/2}$  is a correction factor for a  $\Lambda$ CDM cosmology. We use this fitting function largely to model the precipitous drop in the comoving star formation rate at  $z \sim 1$ ; we choose the normalization factor  $A$  so that  $(1 - R) \int_0^5 \dot{\Omega}_{*} = f_{*}\Omega_{\text{b}} = 2 \times 10^{-3}$ , where  $f_{*} = 5\%$  is the total baryon fraction in stars seen today (Cole et al 2001), as inferred from the K-band luminosity function. They also present two other models which vary the amount of star formation at high redshift; however, we shall see that these variations make little difference to our calculations. To estimate the comoving density of cold gas, we use estimates of the neutral gas in damped Ly-alpha systems (Pefoux et al 2002; Rao & Turnshek 2000), as well as estimates of the local HI density from 21 cm emission surveys (Zwaan, Briggs & Verheijen 2001; Rosenberg & Schneider 2002).

In Figure 6, we show the results of computing  $\Omega_{\text{g}}(z)$  from equation (14). This shows the comoving density of in-

terstellar gas required at redshift  $z$ , if all gas inflow/cooling ceases at that redshift, in order to be consistent with the observed comoving star formation rate as a function of redshift and the local observed gas density. One simple way to phrase this constraint is that  $\Omega_g(z_{\text{preheat}}) \approx \Omega_g(0) + \Omega_*(0) \approx 2 \times 10^{-3} (f_{\text{cool}}/0.05)$ , where  $f_{\text{cool}}$  is the cool global baryon fraction today. We see from the figure that there is sufficient cool gas at high redshift to produce the stars seen today; in particular, preheating at high redshift  $z \sim 2$  can be plausibly accommodated without subsequent gas cooling and inflow. Note that the normalization of  $\Omega_g(z)$  is fixed by the assumed value of  $f_{\text{cool}}(z=0)$  (which is uncertain to at least a factor of 2); if this value increases all the curves shift upward. Also,  $\Omega_{\text{DLA}}$  is obviously merely a lower bound on  $\Omega_{\text{cool}}$ . The surveys are based on optically selected quasars, so dusty damped Ly-alpha systems will not be represented if they dim the background quasar so that it falls out of a magnitude limited survey; also, a significant fraction of the gas could lie in lower column density systems or in molecular or ionized form. Therefore, despite uncertainties in the modelling and data, we can at least conclude that the data do not rule out the absence of gas cooling and inflow into galaxies since  $z \sim 2$ .

### 3 DISCUSSION

#### 3.1 Shock heating of the Warm Hot Intergalactic Medium

Cosmological simulations predict that  $\sim 30-40\%$  of present day baryons reside in a warm-hot intergalactic medium (WHIM), with temperatures  $10^5 < T < 10^7$  K, and mean overdensities  $\delta \sim 10-30$ , rather than in virialized objects (Cen & Ostriker 1999; Croft et al 2001; Davé et al 2001). Can gas heated in such large scale shocks accrete and cool in galaxies? Davé et al (2001) find that the WHIM at  $z=0$  approximately follows the equation of state:  $\rho/\rho_b = T/10^{4.7}$  K. We can use this to estimate the entropy of the WHIM:

$$S_{\text{WHIM}}(z=0) \approx 340 \left( \frac{\delta}{30} \right)^{1/3} \text{ keV cm}^{-2}. \quad (16)$$

Since  $S_{\text{WHIM}} > S_{\text{crit}}$ , none of the gas in the WHIM, even if accreted onto galaxies, can cool in a Hubble time. Thus, shock heating by large scale structure could conceivably play a similar role as preheating in raising the entropy of the IGM and suppressing accretion and gas cooling.

However, in hierarchical structure formation scenarios, such shock heating cannot be responsible for the observed entropy floor in groups and clusters. Shock heating of the WHIM corresponds to  $\sim 1\sigma$  fluctuations turning nonlinear today; the cores of groups and clusters were assembled at high redshift when they were  $> 2\sigma$  fluctuations. Gas shocked in the WHIM phase is likely shocked again as it is boosted to the higher entropies  $S \sim 1350(T/1\text{keV})(n/2 \times 10^{-5}\text{cm}^{-3})^{-2/3} \text{ keV cm}^{-2}$  associated with the outskirts of present-day groups and clusters. Shock heating of the WHIM is likely only to affect gas accretion in voids, where the halos have shallow potential wells and are unable to accrete gas of high entropy.

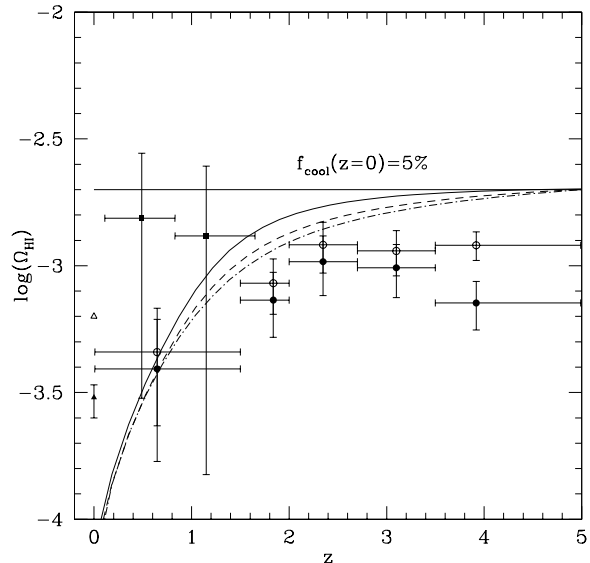


**Figure 6.** The comoving density of interstellar gas required at redshift  $z$ , if all gas inflow/cooling ceases at the redshift, in order to be consistent with the observed comoving star formation rate as a function of redshift, as computed from equations 14 and 15. The curves are normalized to produce the total comoving density of stars seen at  $z=0$ ,  $\Omega_*(0) \approx 2 \times 10^{-3}$ , as inferred from the K-band luminosity function (Cole et al 2001); any increase in this estimate would move the curves upward. The points show the inferred comoving neutral gas density in damped Lyman-alpha systems (Proulx et al 2002; filled circles; open circles denote their correction for gas in lower column density systems), Rao & Turnshek 2000 (filled squares) and seen locally in 21 cm emission (Zwaan et al 2001 (filled triangle), Rosenberg & Schneider 2002 (open triangle)). In general these represent lower limits. There is sufficient cold gas at high redshift to be consistent with a shutoff in gas accretion since  $z \sim 2$ .

We can estimate the redshift evolution of the WHIM entropy as follows. The postshock temperature of the WHIM can be estimated as:

$$T_{\text{WHIM}}(z) = K(HL_{\text{nl}})^2, \quad (17)$$

where  $H(z)$  is the Hubble constant,  $L_{\text{nl}}$  is the nonlinear length scale in proper coordinates; this produces a good fit to the results of numerical simulations (Cen & Ostriker 1999; Davé et al 2001). We have chosen the normalization constant  $K$  so as to reproduce the median temperature for a given overdensity obtained by Davé et al (2001) at  $z=0$ . At a given overdensity  $\delta$ , the entropy of the WHIM scales as  $S_{\text{WHIM}} \propto H(z)^2 L_{\text{nl}}^2 (1+z)^{-2}$ ; it thus falls rapidly with redshift. We plot  $S_{\text{WHIM}}(z)$  in Figure (7); it only exceeds  $S_{\text{crit}}$  at  $z < 1$ . In practice there will be significant scatter about the median entropy of the WHIM (for instance, the temperature distribution broadens at high redshift; see Fig. 4 of Davé et al 2001). It would be interesting to use existing numerical simulations to compute the distribution function of entropy in the WHIM, as well as the redshift evolution of the median IGM entropy; such quantities to date have not been calculated.

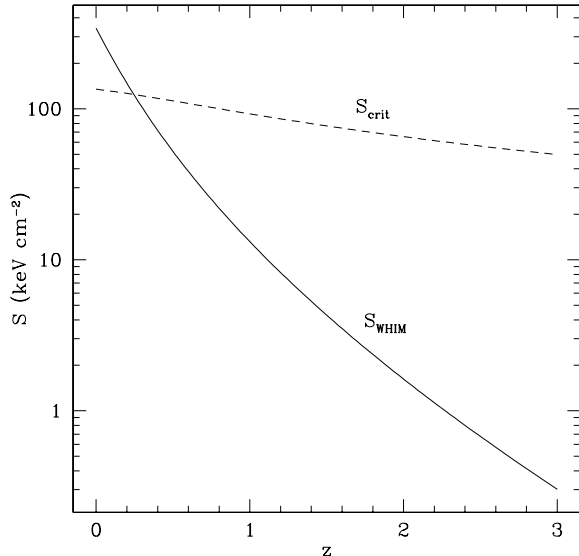


**Figure 7.** The evolution of the median entropy of the WHIM as a function of redshift. Note that  $S_{\text{WHIM}} \propto \delta^{1/3}$ ; here we assume  $\delta \sim 30$ . Although in practice there will be wide scatter about this relation, we nonetheless see that the entropy of the WHIM falls very rapidly with redshift. In particular, it only exceeds the critical entropy  $S_{\text{crit}}$  required to prevent cooling within a Hubble time at late times.

It is amusing to speculate on the effect of a cosmological constant on the future star formation history of our universe. The growth function is given by (Heath 1977):

$$D_1(a) \propto H(a) \int_0^a \frac{da'}{a'^3 H(a')^3}, \quad (18)$$

where  $a = 1/(1+z)$  is the scale factor and  $H(a) = (\Omega_m a^{-3} + \Omega_k a^{-2} + \Omega_\Lambda)^{1/2}$ , where  $\Omega_k = 1 - \Omega_m - \Omega_\Lambda$ . Note that at early times when  $a$  is small,  $D_1(a) \propto a$ . If we normalize this so that  $a = 1$  and  $D_1(0) = 1$  today, then in the future when  $a \rightarrow \infty$ ,  $D_1(a) \rightarrow 1.39$ . Thus, structure formation is already freezing out; the non-linear mass  $M_*$  will increase by at most a factor of 4 from its present day value, in contrast to its rapid growth in the past. Thus, gravitational shock heating is slowing down and becoming unimportant, as the universe enters a period of exponential expansion. Gas in already virialized halos will eventually be able to cool as the universe ages, modulo feedback by star formation and AGN activity fueled by gas cooling. This is in contrast to the  $\Omega_m = 1$  SCDM case, when  $D_1 = a$  and structure formation and gravitational shocks continue apace; in this case most of the non-stellar baryons in the universe would end up in a hot phase which will never cool.

### 3.2 Could Preheating determine Galaxy Morphology?

We speculate that preheating may be responsible for the origin of the Hubble sequence. Gas in dark matter halos which form before the epoch of preheating are assumed to form

an elliptical galaxy in a rapid collapse, since halos below group scales have gas with cooling times shorter than their dynamical time  $t_{\text{cool}} < t_{\text{ff}}$  (Rees & Ostriker 1977). On the other hand, halos which collapse after preheating will accrete gas with entropies more characteristic of groups and clusters; in particular, they can cool their gas only slowly, with  $t_{\text{cool}} > t_{\text{ff}}$ . Cooling gas in such halos may instead form a disk galaxy. In fact, Mo & Mao (2002) point out that preheating could potentially solve two problems associated with disk galaxies: explaining the anomalously low X-ray surface brightnesses associated with their halos (since preheating decreases gas densities and X-ray emissivities), and preventing angular momentum transport from the disk to the dark matter during disk formation (because the gas distribution is more extended than that of the dark matter, it retains a higher specific angular momentum during mergers). We note in passing that the low X-ray luminosities of halos associated with disks is perhaps unsurprising: a simple extrapolation of the  $L_X - T_X$  relation to halo temperatures typical for the hosts of disks ( $\sim 0.1\text{keV}$ ) gives X-ray luminosities consistent with observations ( $\text{few} \times 10^{40} \text{erg s}^{-1}$ ). Thus, whatever physics is suppressing the X-ray luminosities of group operates in disk galaxies too.

In a hierarchical formation scenario, the progenitors of massive clusters typically formed earlier than those of lower mass systems. Thus, massive clusters contain a larger fraction of galaxies which formed prior to the epoch of preheating; the fraction of elliptical galaxies should increase as the mass of the dark matter halo increases. To compute this fraction of galaxies which formed before preheating (and therefore formed ellipticals) we create merger trees for halos of different masses at  $z = 0$ . We then identify when  $10^{12} M_\odot$  progenitor halos form in these trees. If the progenitor formed before preheating (assumed to occur at  $z = 2$  here) the halo is flagged as hosting an elliptical galaxy, while halos which collapse later are assumed to host a disk galaxy. In Figure 8 we show the fraction of galaxies formed in  $10^{12} M_\odot$  halos which are ellipticals as a function of the mass of the halo in which they are found at  $z = 0$ . This is compared against the observational determinations of Balogh et al (2002) of the elliptical fraction (shown as circles), with their estimate of the “field” elliptical fraction shown as a dashed line. Our simple calculation fits rather well with these data (note that the “field” should correspond approximately to  $M_* \sim 10^{13} h^{-1} M_\odot$  halos). Since the typical mass of halos increases in denser environments we expect this model to produce the observed morphology-density relation, at least qualitatively. A direct comparison requires a detailed model of galaxy formation, since it requires calculating the local galaxy density within the model.

This is of course little more than a consistency check, rather than proof of principle. The idea that ellipticals collapsed at much higher redshift than spirals is an old one. It was suggested long ago that there may be a direct correspondence between peak height and galaxy morphology, with ellipticals forming from rare ( $\sim 3\sigma$ ) density fluctuations, while spirals form from more common ( $\sim 2\sigma$ ) ones (Blumenthal et al 1984; Evrard 1989); such a scheme can reproduce their observed relative abundances fairly well and would also ex-



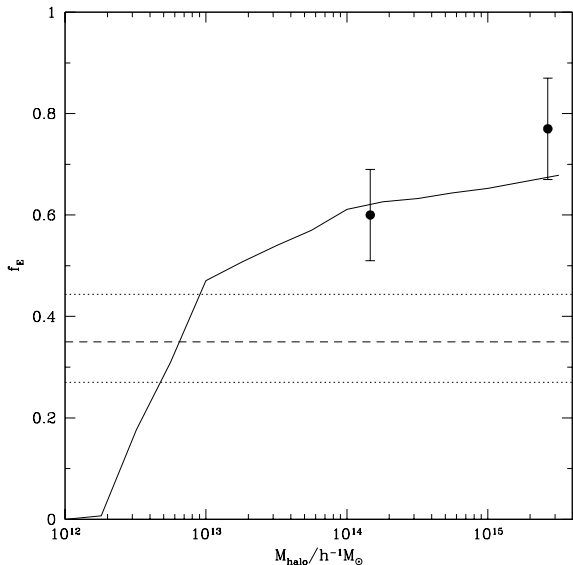


**Figure 8.** The fraction of galaxies formed in  $10^{12}M_{\odot}$  halos which are ellipticals, as a function of the mass of the halo in which they are found at  $z = 0$ . Points with errorbars show the determinations of Balogh et al (2002). (The X-ray luminosities of clusters in Balogh et al (2002) were converted to cluster virial masses using the relation of Reiprich & Böhringer (1999).) The dashed line shows the “field” elliptical fraction from Balogh et al (2002), with dotted lines showing their errorbars.

plain the increased clustering strength of ellipticals. Empirically, it is known that ellipticals exhibit remarkably tight correlations in various global properties and have very small inferred age dispersion which indicate a high formation redshift  $z \sim 2 - 3$ , unless their formation was synchronized to an implausible degree. The evidence includes the tightness of the fundamental plane (van Dokkum et al 1998), and the extreme homogeneity of their optical colors (Bower, Lacey & Ellis 1992; Ellis et al 1998). However, the physical motivation for early formation of ellipticals rather than spirals has been rather weak.

The interesting feature that preheating introduces is a physical reason why there should be a division in morphology between early and late collapse of halos of the same mass, because of the change in the cooling properties of the gas. There may be some critical level of entropy (likely  $t_{\text{cool}}(S_{\text{crit}}) \sim t_{\text{dyn}}$ ) where galaxy formation switches from one mode to another. To test these speculations, it would be necessary to conduct high resolution simulations of a single galaxy, to observe how galaxy morphology and disk structure changes as the entropy of the accreted gas is increased. To some extent, we know already from previous simulations (based on suggestions that photo-ionization could delay cooling until  $z \sim 1$ ) that feedback processes which delay gas cooling result in less angular momentum transfer and more disk-like features (Weil, Eke & Efstathiou 1998).

Preheating may also help alleviate possible problems with the dearth of galaxies found in voids (Peebles 2001; Mathis & White 2002; Benson et al 2002). Since the dis-

tribution of halo masses in voids is shifted to lower masses relative to the field, preheating will be particularly effective in suppressing galaxy formation in these environments. However, lower mass halos also tend to collapse earlier, so a larger fraction of these halos will form prior to preheating. This latter effect seems to dominate. Using dark matter halos from the simulations of Benson et al (2002), we identified halos which formed after preheating at  $z = 2$  (assuming the distribution of formation redshifts given by Verde et al. (2001) and no correlation of formation time with environment). Removing these halos from the sample makes only minor differences to the void probability function for example. Although these simulations have a rather poor mass resolution for the study of void galaxies, we expect the effects of preheating to become even less for lower mass halos, since an even greater fraction of these should form prior to preheating.

### 3.3 Conclusions

In this paper, we stress that radiative cooling alone cannot account for the observed entropy floor in clusters and the minimum entropy required to produce the observed deviation from self-similarity in the  $L_X - T_X$  relation. This is only possible with severe overcooling. Thus, some form of entropy injection—perhaps through supernovae or AGN winds—seems necessary (though radiative cooling still plays a very important role in reducing the energetic requirements for producing an entropy floor (Voit et al 2002)). The level of entropy injection required to produce observable changes in the density profiles of deep potential wells of groups and clusters must have a drastic effect on smaller halos which host galaxies. We show that entropy injection can indeed play a very important role in regulating gas accretion and cooling in galaxies, since gas heated to the entropy floor can never cool in a Hubble time, regardless of the densities it is compressed to: for gas temperatures typical of galaxy halos the cooling time depends almost exclusively on entropy and is relatively independent of density. Thus, after the epoch of preheating, the gas supply to galaxies was cut off. This is not inconsistent with observations if an epoch of preheating at  $z \sim 2$  is assumed. We speculate that at a critical level of entropy  $t_{\text{cool}}(S_{\text{crit}}) \sim t_{\text{ff}}$ , the mode of gas collapse changes from free-fall and fragmentation (which produces ellipticals) to quiescent accretion (which produces spirals).

There are many aspects of the impact of preheating on galaxy formation which would be worth pursuing in greater detail, particularly with numerical simulations. One would be the redshift and spatial dependence of entropy injection—we have only considered a uniform level of entropy injection which appears instantaneously at  $z \sim 2$ . Naively, we would expect entropy injection to be proportional to the integrated star formation, which is proportional to the local stellar density and local metallicity. Similarly, the spatial variation and distribution function of entropy due to shock heating of the IGM deserves attention, and the possibility that the entropy of the IGM may be responsible for galaxy morphology. It may well be that the entropy of the IGM regulates the amount of cooling and star-formation at any

given cosmological epoch, and is the chief mechanism which prevents overcooling at high redshift.

## ACKNOWLEDGMENTS

We thank Celine Peroux for providing the data used in Fig 6, and Jerry Ostriker (long ago) and Tommaso Treu for helpful discussions.

## REFERENCES

- Balogh, M.L., Pearce, F.R., Bower, R.G., & Kay, S.T., 2001, MNRAS, 326, 1228
- Balogh, M.L., Smail, I., Bower, R.G., Ziegler, B.L., Smith, G.P., Davies, R.L., Gaztelu, A., Kneib, J.-P., Ebeling, H., 2002, ApJ, 566, 123
- Benson, A.J., Hoyle, F., Torres, F., Vogeley, M.S., 2002, MNRAS in press
- Bell, E.F., & de Jong, R.S., 2000, MNRAS, 312, 497
- Blumenthal, G.R., Faber, S.M., Primack, J.R., & Rees, M.J., 1984, Nature, 311, 517
- Bower, R.G., Lacey, J.R., & Ellis, R.S., 1992, MNRAS, 254, 589
- Bryan, G.L., 2000, ApJ 544, L1
- Cavaliere, A., Menci, N., & Tozzi, P., 1997, ApJ, 484, L21
- . 1998, ApJ, 501, 493
- Cen, R., & Ostriker, J.P., 1999, ApJ, 519, L109
- Cole, S., Lacey, C.G., Baugh, C.M., Frenk, C.S., 2000, MNRAS, 319, 168
- Cole, S., et al, 2001, MNRAS, 326, 255
- Croft, R.A.C., Ci Matteo, T., Davé, R., Hernquist, L., Katz, N., Fardal, M.A., & Weinberg, D.H., 2001, ApJ, 557, 67
- Davé, R., Cen, R., Ostriker, J.P., Bryan, G.L., Hernquist, L., Katz, N., Weinberg, D.H., Norman, M.L., & O’Shea, B., 2001, ApJ, 552, 473
- Davé, R., Katz, N., & Weinberg, D.H., 2002, ApJ, 579, 23
- Ellis, R.S., et al, 1998, ApJ, 483, 582
- Evrard, A.E., 1989, ApJ, 1989, 341, 26
- Finoguenov, A., Jones, C., Bohringer, H., & Ponman, T.J., 2002, ApJ, 578, 74
- Freedman, W.L., et al., 2001, ApJ, 553, 47
- Fukugita, M., Hogan, C.J., & Peebles P.J.E., 1998, ApJ, 503, 518
- Ghigna, S., Moore, B., Governato, F., Lake, G., Quinn, T., Stadel, J., 2000, ApJ, 544, 616
- Heath, D.J., 1977, MNRAS, 179, 351
- Helsdon, S.F., Ponman, T.J., 2000, MNRAS, 315, 256
- Kaiser, N., 1986, MNRAS, 222, 323
- Kaiser, N., 1991, ApJ, 383, 104
- Klypin, A., Kravtsov, A.V., Bullock, J.S., Primack, J.R., 2001, ApJ, 554, 903
- Landau, L.D., & Lifshitz, E.M., 1959, in Fluid Mechanics (London: Pergamon Press), 329
- Lewis, G.F., Babul, A., Katz, N., Quinn, T., Hernquist, L., & Weinberg, D.H., 2000, ApJ, 536, 623
- Mathis, H., White, S.D.M., 2002, MNRAS in press
- Mo, H.J., Mao, S., 2002, MNRAS, 333, 768
- Muanwong, O., Thomas, P.A., Kay, S.T., & Pearce, F.R., 2002, MNRAS, 336, 527
- Mulchaey, J.S., Davis, D.S., Mushotzky, R.F., & Burstein, D., 1996, ApJ, 456, 80
- B.B., 2002, MNRAS in press, astro-ph/0201410
- Navarro, J.F., Frenk, C.S., & White, S.D.M., 1997, ApJ, 490, 493
- Netterfield, C.B., et al., 2002, ApJ, 571, 604
- Peebles, P.J.E., astro-ph/0101127
- Pei, Y.C., Fall, S.M., & Hauser, M.G., 1999, ApJ, 522, 604
- Pefoux, C., McMahon, R.G., Storrie-Lombardi, L.J., & Irwin, M.J., MNRAS, submitted, astro-ph/0107045
- Ponman, T.J., Cannon, D.B., & Navarro, J.F., 1999, Nature, 397, 135
- Porciani, C., & Madau, P., 2001, ApJ, 548, 522
- Power, C., Navarro, J.F., Jenkins, A., Frenk, C.S., White, S.D.M., Springel, V., Stadel, J., Quinn, T., 2002, astro-ph/0201544
- Rao, S.M., & Turnshek, D.A., 2000, ApJ, 130, 1
- Rees M. J., Ostriker J. P., 1977, MNRAS, 179, 541
- Reiprich, T.H., Böhringer, H., 1999, Astron. Nachr., 320, 296
- Rosenberg, J.L., & Schneider, S.E., 2002, ApJ, 567, 247
- Roussel, H., Sadat, R., & Blanchard, A., 2000, A&A, 361, 429
- Smith, G.P., Edge, A.C., Eke, V.R., Nichol, R.C., Smail, I., Kneib, J.-P., 2002, astro-ph/0211186
- Suginohara, T., & Ostriker, J.P., 1998, ApJ, 507, 16
- Sutherland, R.S., & Dopita, M.A., 1993, ApJS, 99, 253
- Tozzi, P., & Norman, C., 2001, ApJ, 546, 63
- van Dokkum, P.G., Franx, M., Kelson, D.D., & Illingworth, G., 1998, 1998, ApJ, 504, L17
- Verde, L., Kamionkowski, M., Mohr, J., Benson, A.J., 2001, MNRAS, 321, L7
- Voit, G.M., & Bryan, G.L., 2001, Nature, 414, 425
- Voit, G.M., Bryan, G.L., Balogh, M.L., Bower, R.G., 2002, ApJ, in press, astro-ph/0205240
- Weil, M.L., Eke, V.R., & Efstathiou, G., 1998, MNRAS, 300, 773
- White, S.D.M. & Frenk, C.S., 1991, ApJ, 379, 52
- Wu, X.-P., & Xue, Y.-J., 2002, ApJ, 572, L19
- Zwaan, M., Briggs, F., Verheijen, M., 2001, in Extragalactic Gas at low redshift, eds. Mulchaey et al., astro-ph/0108498